FABRICATION OF PhC STRUCTURES BY USING NANOIMPRINT LITHOGRAPHY AND THEIR OPTICAL PROPERTIES

Juraj Nevřela
PhD Student[1]
juraj.nevrela@stuba.sk

Anton Kuzma
PhD[1]
antom.kuzma@stuba.sk

[1]*Faculty of Electrical Engineering and Information*
Institute of Electronics and Photonics
Slovak University of Technology in Bratislava
3 Ilkovicova str., Bratislava, Slovakia, 812 19

Abstract: The contribution deals with creating structure, which have unique properties for influencing the spectrum of light. Since these structures exhibit the period under the diffraction limit of visible light or UV radiation, they can't be fabricated by standard photolithography. As a result, this nanoscale structure must be prepared with progressive nanostructure patterning technology known as nanoimprint lithography (NIL). Especially, in our work UV-nanoimprint lithography was used. Considering preservation of low production costs, which plays a crucial role in the industry, the UV-nanoimprint lithography will be best suit for this purpose. Using this technology result with respect to reproducibility and uniformity of created nanostructure has been achieved. Ability of influencing light spectrum for nanostructures with the period of 800 nm and 600 nm with various feature size were presented with observation and simulation also.

Keywords: PhC, nanostructure, NIL, hard stamp, UV-exposure, next generation of nanoscale lithography, RCWA, LED, RIE, AFM.

1. Introduction

In the recent years, it has been shown that the light outcoupled from the LED source can be enhanced. This can be done in several ways. Adding double heterojunction, or quantum wells to LEDs chip during the processing are few to mention. Even though they may enhance the light outcoupled, all-new layout of the chip is often required, which leads to increase of production costs that also reflects on the market cost. Another possibility is influencing the management of light by adding Photonic crystals. PhC structure on the chip doesn't require any changes in the layout. Photonic crystals are used in applications where the management of light has to be influenced. This is a feature that makes them suitable for use in modern photonics. PhCs are commonly applied to the surface of inorganic LEDs to increase efficiency of emitted light. PhC structures create a forbidden optical band that prevents photons from propagating to the frequency falling within that band. The result is an increase in photon extraction in the vertical direction from LED [1, 2]. Considering to the size of the PhC structures a reliable method of producing them is needed while maintaining a low price.

As a consequence, there is a need for the next generation of nano-scale lithography (NGL) technique. Recently, the technique of nanoscale pattern transfer technology using a mold, has attracted attention, thanks to the possible technology and know-how transfer from academical soil to industry, as well as high technology readiness levels (TRL) [3]. Considering preservation of low production costs, which plays a crucial role in organic electronics market penetration, the nanoimprint lithography (NIL) may be the best suited for this purpose. Nanoimprint lithography is one of the advanced fabrication technologies and possibly may become the fabrication technology in electronics and optoelectronics industry [4–10]. The greatest advantage of these processes lies in higher production yield as well as in better cost-effectiveness compared to other NGL techniques, such as electron beam lithography.

2. Material and Methods

The quartz glass stamp was used in nanoimprint lithography. Stamp consists of different patterns at several locations, as shown in **Fig. 1.** Each group (square) of patterns in the column has a constant width of lines (higher parts in the pattern) marked as w. pitch (period) of a structure is changed for each square in **Fig. 1.**

Nanostructures were prepared on Si substrates with 120 nm SiO_2. Nanostructures were fabricated by nanoimprint lithography, and therefore absolute purity of the substrate is necessary. Substrate cleaning was realized with following steps. First of all samples were cleaned with acetone and isopropyl alcohol in order to remove organic impurities. After these steps, it was treated with DMI water in ultrasonic bath. The last step was treatment in oxygen plasma for removing residual organic materials from surface.

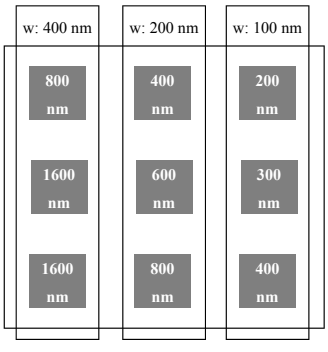

Fig. 1. Schematic patterns of stamp

For creating nanostructure Suss Microtec MA6 mask aligner, as well mr UVCur21 from Micro resist technology was used. For pattern transfer from photoresist to SiO_2 Oxfor Plasmalab system 100 was used.

3. Results

In **Fig. 2, *a*, *c*** is shown topology of fabricated nanostructure using above mentioned stamp, specifically a 1D PhC structure with 400 nm thick lines, 800 nm pitch, and 200 nm thick lines, 600 nm pitch. A XE-100 Park systems atomic force microscope was employed for acquiring the AFM scanning from nanoimprinted patterns. Inhomogeneity was observed on surface of fabricated structure, caused by the adhesive forces between a stamp and photoresist during separation. The height of the lines was estimated to 52–54 nm using statistical function as shown in **Fig. 2, *b*, *d***. The nano-pillars of the patterned area on the stamp shows a height in average 56 nm (50 nm declared by datasheet).

In the next step nanostructure was transferred to the SiO_2 with the dry etching process. First of all residual photoresist layers (from the bottom of the structure) was removed by oxygen powered RIE. Dry anisotropic etching of SiO_2 has been achieved with CF4 gas. The chamber was evacuated to the 5 mtTorr and flow of working gas to the 20 sccm. Self-bias voltage was set to the 200 V. Etch rate was estimate to the 10 nm per minute. Topology of etched structure is shown in **Fig. 3, *a***. The statistic function was applied to calculate the height of nanostructure which is in average 34 nm. The statistic function is shown in **Fig. 3, *b***. Surface roughness after etching was estimated on 3 nm at the bottom and 4,2 nm at the top of structure, which are comparable to roughness before this technological step.

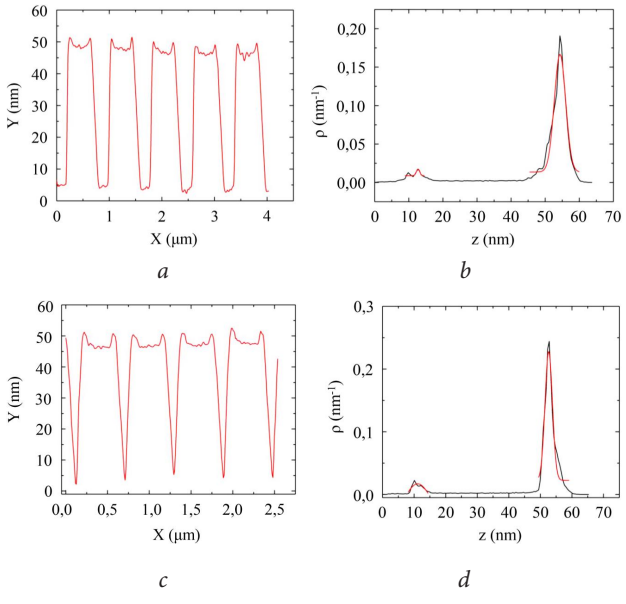

Fig. 2. AFM analysis of molded structure**:** *a* – Topology of molded structure with period 800 nm and 400 nm width hole; *b* – Statistic function for period 800 nm; *c* – Topology of molded structure with period 600 nm and 200 nm width hole; *d* – Statistic function for period 600 nm

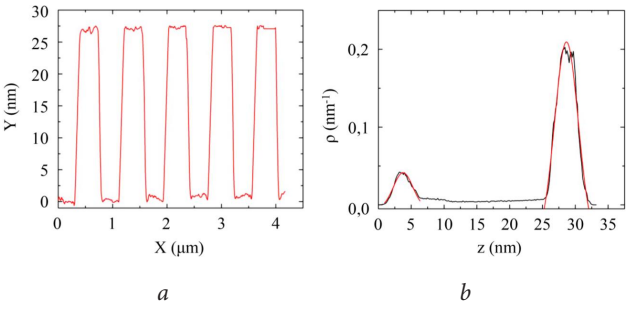

Fig. 3. AFM analysis of structure**:** *a* – Topology of structure etched to the surface (period 800 nm); *b* – Statistic function

4. Discussion and conclusions

Top and side illumination (under 30 degrees of the incident light) was used during the investigation of the samples. In the **Fig. 4** is shown the light reflected from the top of the sample. This photo was taken by a microscope camera situated above the sample surface, in the long working distance (10 cm).

The structure was designed in RSoft's Photonic Component Design Suite [9]. The material parameters of the layers described in Palik [10] were applied. The rigorous coupled-wave analysis (RCWA) simulation method was used for the simulations of the structure including 1D pattern in the layer. Even though the structure is designed as a 1D layer with patter, 2D simulations were performed by the RCWA simulation method. This simulation method is best suitable for calculating transmission, reflection and absorption of incident radiation in the examined structure throughout whole spectrum of wavelengths and in all angles. It may help in recognizing increase in extraction efficiency or a change of output characteristics of Simulations as well as optical investigation show diffraction effects of patterns with higher periods for wavelengths from the visible light spectrum. Lower periods cause diffraction effects for radiation in the UV spectrum. **Fig. 5**, **6** are illustrated reflectance as a function of an angle of incidence of illuminated light for samples reflected yellow (400×800) and cyan (200×800) light underside illumination. Reflectances are illustrated as a contour map rescaled to the max value of the visualized range of angle of incident and wavelength. Investigation of reflectance over the spectrum is an evident match between imaged camera images and simulated results.

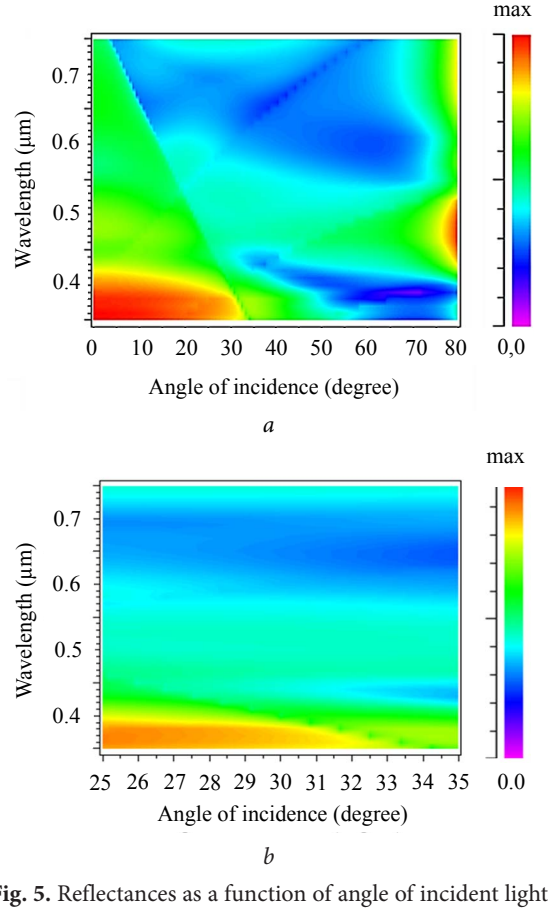

Fig. 5. Reflectances as a function of angle of incident light from visible spectrum for nanostructure with 800 nm period and feature size of 400 nm: *a* – Reflectances for a broad range of angle of incidence; *b* – Reflectances for a range of angle of incidence corresponding to side illumination

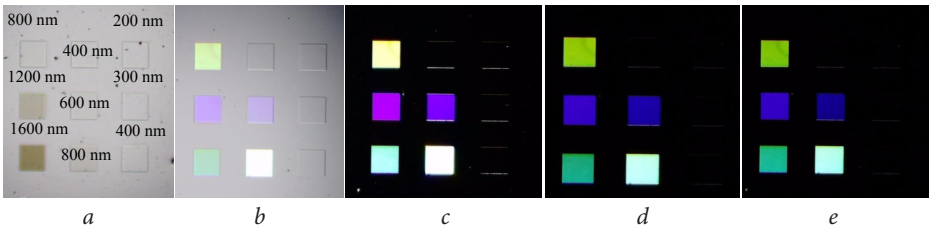

Fig. 4. Reflected light from structures of the imprint: *a* – Top illumination and period of each square; *b* – Top and side illumination under 30°; *c* – Side illumination under 30°; *d* – Side illumination under 30°– TM mode; *e* – Side illumination under 30° – TE mode

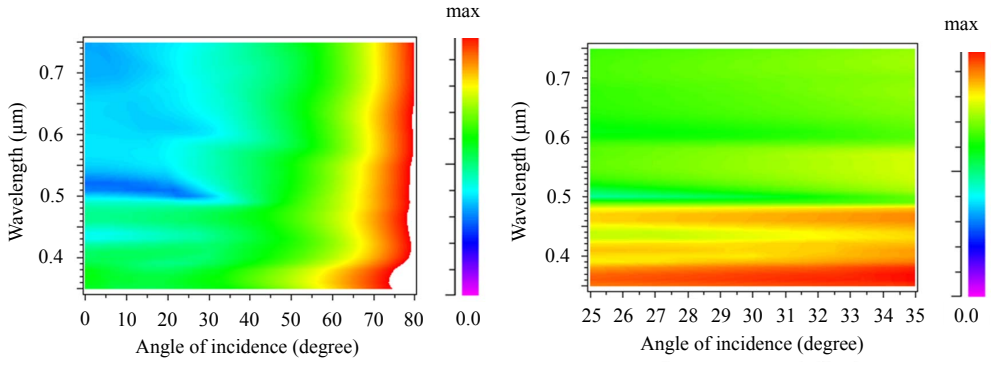

a *b*

Fig. 6. Reflectances as a function of angle of incident light from visible spectrum for nanostructure with 800 nm period and feature size 200 nm: *a* – Reflectances for a broad range of angle of incidence; *b* – Reflectances for a range of angle of incidence corresponding to side illumination

Acknowledgement

This work was supported by Slovak Research and Development Agency under projects No. APVV-17-0522 and APVV-17-0501.

References

1. Joannopoulos, J. D., Johnson, S. G., Winn, J. N., Meade, R. D. (2011). Photonic Crystals. Princeton University Press. doi: https://doi.org/10.2307/j.ctvcm4gz9
2. Hua, F., Sun, Y., Gaur, A., Meitl, M. A., Bilhaut, L., Rotkina, L. et. al. (2004). Polymer Imprint Lithography with Molecular-Scale Resolution. Nano Letters, 4 (12), 2467–2471. doi: https://doi.org/10.1021/nl048355u
3. Zhou, W. (2012). Principles and Status of Nanoimprint Lithography. Nanoimprint Lithography: An Enabling Process for Nanofabrication, 5–32. doi: https://doi.org/10.1007/978-3-642-34428-2_2
4. Roco, M. C., Hersam, M. C., Mirkin, C. A. (2011). Nanotechnology Research Directions for Societal Needs in 2020. Springer. doi: https://doi.org/10.1007/978-94-007-1168-6
5. Chou, S. Y., Keimel, C., Gu, J. (2002). Ultrafast and direct imprint of nanostructures in silicon. Nature, 417 (6891), 835–837. doi: https://doi.org/10.1038/nature00792
6. Kim, E., Xia, Y., Whitesides, G. M. (1995). Polymer microstructures formed by moulding in capillaries. Nature, 376 (6541), 581–584. doi: https://doi.org/10.1038/376581a0
7. Hirai, Y., Tanaka, Y. (2002). Application of Nano-imprint Lithography. Journal of Photopolymer Science and Technology, 15 (3), 475–480. doi: https://doi.org/10.2494/photopolymer.15.475
8. Mühlberger, M., Bergmair, I., Schwinger, W., Gmainer, M., Schöftner, R., Glinsner, T. et. al. (2007). A Moiré method for high accuracy alignment in nanoimprint lithography. Microelectronic Engineering, 84 (5-8), 925–927. doi: https://doi.org/10.1016/j.mee.2007.01.081
9. Rsoft Design Group, Inc., RSoftPhotonics CAD Layout User Guide, 200. Executive Blvd., Ossining, NY: Physical Layer Division (2013).
10. Palik, E. (1997). Introductory Remarks. Handbook of Optical Constants of Solids, 3–12. doi: https://doi.org/10.1016/b978-012544415-6/50097-2

Received date 09.10.2019
Accepted date 05.11.2019
Published date 23.11.2019